

# Advanced Pitch Angle Control Based on Fuzzy Logic for Variable-Speed Wind Turbine Systems

Tan Luong Van, *Member, IEEE*, Thanh Hai Nguyen, *Member, IEEE*, and Dong-Choon Lee, *Senior Member, IEEE*

**Abstract**—In this paper, an advanced pitch angle control strategy based on the fuzzy logic is proposed for the variable-speed wind turbine systems, in which the generator output power and speed are used as control input variables for the fuzzy logic controller (FLC). The pitch angle reference is produced by the FLC, which can compensate for the nonlinear characteristic of the pitch angle to the wind speed. With the control variables of the generator output power and speed, the wind turbine is smoothly controlled to maintain the aerodynamic power and its speed at the rated values without any fluctuation in the output power and speed in the high-wind-speed regions. The effectiveness of the proposed method is verified by simulation results for a 2-MW permanent-magnet synchronous generator (PMSG) wind turbine system, and experimental results for a reduced-scale PMSG wind turbine simulator.

**Index Terms**—Fuzzy logic controller (FLC), gain scheduling, pitch angle control, permanent-magnet synchronous generator (PMSG), wind turbine.

## I. INTRODUCTION

RECENTLY, the renewable energy, especially wind energy, has been paid much attention due to the energy shortage and environmental concern. As the penetration of the wind energy into the electrical power grid is extensively increased, the influence of the wind turbine systems on the frequency and voltage stability becomes more and more significant [1]–[4]. Consequently, the power control technique of the wind turbines is also getting more important in the view point of grid integration.

The variable-speed, variable-pitch wind turbine systems typically have two operating regions according to the wind speed. In the partial-load region where the wind speed is lower than the rated-wind speed  $v_{\text{rated}}$ , the turbine speed is controlled at the optimal value so that the maximum energy is extracted from the wind turbine [5], [6]. In the full-load region where the wind speed exceeds its rated value, the generator output power is limited at the rated value by controlling the pitch angle since the capacity of the generator and converter are limited [7]–[9]. On the contrary, the pitch regulation can be used for output power smoothening at the partial-load region [10], [11].

Manuscript received May 6, 2014; revised September 8, 2014; accepted November 25, 2014. Date of publication January 23, 2015; date of current version May 15, 2015. This work was supported by the Basic Science Research Program through the National Research Foundation of Korea (NRF) funded by the Ministry of Education (2009-0077374). Paper no. TEC-00308-2014.

T. L. Van is with the Department of Electrical and Electronics Engineering, Sai Gon University, Ho Chi Minh 84-8, Vietnam (e-mail: luongees2@yahoo.com).

T. H. Nguyen and D.-C. Lee are with the Department of Electrical Engineering, Yeungnam University, Gyeongbuk 712-749, Korea (e-mail: nthai@ctu.edu.vn; dclee@yu.ac.kr).

Color versions of one or more of the figures in this paper are available online at <http://ieeexplore.ieee.org>.

Digital Object Identifier 10.1109/TEC.2014.2379293

For limiting the aerodynamic power captured by the wind turbine at the high-wind speed regions, several pitch angle control methods have been suggested. The proportional–integral (PI) or proportional–integral–derivative (PID) based-pitch angle controllers have been often used for the power regulation [1], [12]–[15]. The disadvantage of this method is that the control performance is deteriorated when the operating points are changed since the controller design is based on the turbine model which is linearized at the operating points by a small signal analysis. Another scheme using the  $H_\infty$  controller with a linear matrix inequality approach was proposed [16], which gives a good performance of the turbine output power as well as the robustness to the variations of the wind speed and the turbine parameters. However, it is rather complex since the parameters of the model and the controller need to be redesigned due to the changes of the weighting functions by the constraints.

The linear quadratic Gaussian (LQG) method for the design of the pitch angle control has been applied [17], [18]. It is known that the LQG controller provides robustness in terms of the phase and gain margins. However, the performance of this linear controller is limited due to the highly nonlinear characteristics of the wind turbines.

A pitch angle controller applying the generalized predictive control (GPC) method has been proposed in a wide operating region of the wind speed [10]. With this method, the error of the control signal is minimized in each interval and its divergence is eliminated by minimizing the performance index. However, if there is a large error in the output power, the control system will be unstable since the GPC law depends heavily on the output power error. To solve this problem, the standard deviation of the output power from the wind farm is corrected by the fuzzy reasoning, which can also respond to the rapid changes of the wind speed. However, if the difference between the cut-in wind speed and its rated value is large, the output power fluctuations will increase. Also, to obtain the output power reference, the information of the wind speed is required.

On the other hand, the gain scheduling control has been presented for compensating for the system nonlinearity [19], [20], where the controller gains are continuously updated with the change of the system operating conditions. This control method does not require any online parameter estimation, and provide a relatively fast response to the changes of operating conditions. A major drawback of this method is that the performance depends on the model of the wind turbines linearized at the specific operating points. Also, it is not so easy to design the scheduling function updating the controller gains at the different operating points.

Another method applying a sliding-mode control scheme has been used for the pitch angle control [21], which provides a

good robustness to parametric uncertainties of the wind turbine. However, this method depends on the mathematical model of the wind turbines. In addition, if there is a sudden and large change of the control variables, it leads to the high mechanical stress for the wind turbine system and increases the chattering phenomena.

On the other hand, a few methods using the fuzzy logic control have been proposed for the pitch angle control [22], [23]. These methods are reliable and robust to the nonlinear characteristics of the pitch angle with the wind speed. In [21], there is a disadvantage that the information of the wind speed is required. Using the anemometer increases the cost and degrades the reliability of the system [24]. In addition, both methods have not shown the feasibility of the hardware implementation.

In this paper, a new pitch angle control strategy based on the fuzzy logic control is proposed for limiting the turbine output power and the generator speed in the full-load region. For the fuzzy inputs, the generator output power and the generator speed instead of the wind speed are adopted, which eliminates the use of an expensive anemometer. In addition, with the control variables of the generator output power and speed, the wind turbine is well controlled to maintain the output power and its speed at the rated values without the ripple components. The simulation results for a 2-MW permanent-magnet synchronous generator (PMSG) wind turbine system and the experimental results for a reduced-scale wind turbine simulator show the effectiveness of the proposed method.

## II. WIND TURBINE SYSTEMS

### A. Modeling of Wind Turbines

The turbine torque can be expressed as [1]

$$T_t = \frac{1}{2} \rho \pi R^3 \frac{C_p(\lambda, \beta)}{\lambda} v_w^2 \quad (1)$$

where  $\rho$  is the air density ( $\text{kg/m}^3$ ),  $R$  is the radius of blade (m),  $v_w$  is the wind speed (m/s),  $\beta$  is the pitch angle, and  $\lambda$  is the tip-speed ratio. The power conversion coefficient  $C_p$  is expressed as follows:

$$C_p(\lambda, \beta) = c_1 \left( c_2 \frac{1}{\lambda} - c_3 \beta - c_4 \beta^x - c_5 \right) \exp \left( -c_6 \frac{1}{\lambda} \right) \quad (2)$$

where

$$\frac{1}{\lambda} = \frac{1}{\lambda + 0.08\beta} - \frac{0.035}{1 + \beta^3}$$

and  $c_1 = 0.5$ ,  $c_2 = 116$ ,  $c_3 = 0.4$ ,  $c_4 = 0$ ,  $c_5 = 5$ ,  $c_6 = 21$ , and  $x = 0$  [25].

Fig. 1 shows the power coefficient curves of the wind turbine as a function of the tip-speed ratio and pitch angle.

### B. Pitch Servo

The pitch angle control is usually applied to limit the turbine output power in the medium to large wind turbines. The actuator can adjust the rotation of the blades around the longitudinal axes. The hydraulic or electromechanical devices are widely used for the pitch actuator in the high power range of the turbines.

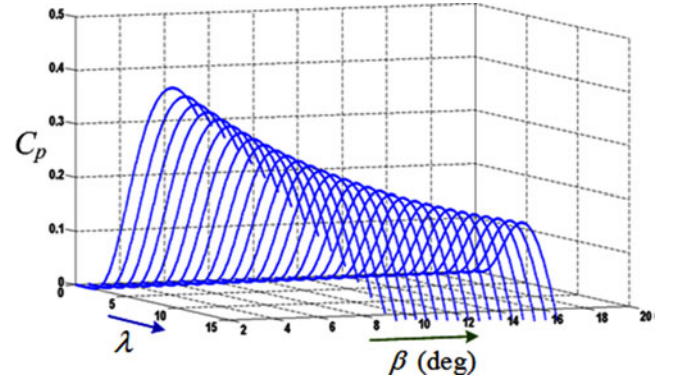


Fig. 1. Power coefficient curves.

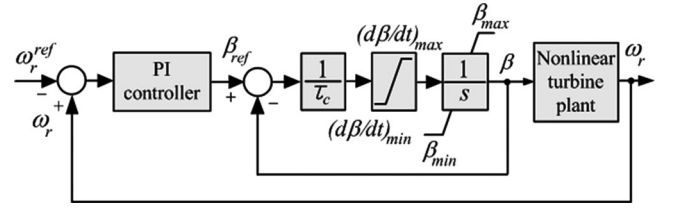


Fig. 2. Block diagram of the typical pitch angle control system.

The pitch actuator is a nonlinear servo that generally rotates all of the blades or a part of them. In the closed loop, the pitch servo is modeled as an integrator or a first-order delay system with a time constant ( $\tau_c$ ). The dynamic behavior of the pitch servo is expressed as [1]

$$\frac{d\beta}{dt} = -\frac{1}{\tau_c} \beta + \frac{1}{\tau_c} \beta_{ref} \quad (3)$$

which is subject to

$$\beta_{min} \leq \beta \leq \beta_{max} \\ \left( \frac{d\beta}{dt} \right)_{min} \leq \frac{d\beta}{dt} \leq \left( \frac{d\beta}{dt} \right)_{max}$$

where  $\beta_{min}$  and  $\beta_{max}$  are the minimum and maximum pitch angles, respectively.

The block diagram of the typical pitch control system is shown in Fig. 2, in which the pitch servo is included. The response of the pitch control depends on the time constant of the pitch actuator, which is normally in range of 0.2-0.25 s [20]. Also, the rate limiter represents a realistic response of the pitch servo. As the pitch rate ( $d\beta/dt$ ) is faster, the transient performance is better. Typically, the  $\beta$  ranges from  $-2$  to  $30$  degrees and varies at the maximum rate of  $\pm 10^\circ \text{s}^{-1}$  [23]. Thus, the rate of change and the variable range in the pitch angle have the considerable effects on the performance of the power regulation. To decrease the risks of the fatigue damage, these limits are not reached during the normal operation of the wind turbine.

### C. Nonlinear Characteristics of Pitch System

The generator speed in the one-mass model of the wind turbine systems is expressed as

$$\frac{d\omega_r}{dt} = \frac{1}{J_g} (T_t - T_g) \quad (4)$$

where  $J_g$  is the combined moment inertia of the turbine and generator, and the generator torque is expressed as

$$T_g = \frac{P_g}{\omega_r} \quad (5)$$

where  $P_g$  is the generator power.

By taking the time derivative of (4), the pitch angle reference  $\beta_{\text{ref}}$  is obtained as [26]

$$\beta_{\text{ref}} = a_1 (a_2 + a_3 + a_4 + a_5 + a_6) \quad (6)$$

where

$$\begin{aligned} a_1 &= \frac{\tau_c J_g \omega_r}{0.5 \rho \pi R^2 v_w^3} \left( \frac{dC_p}{d\beta} \right)^{-1} \\ a_2 &= \frac{0.5 \rho \pi R^2 \beta v_w^3}{\tau_c J_g \omega_r} \frac{dC_p}{d\beta} + \frac{1}{J_g \omega_r} \frac{dP_g}{dt} - \frac{P_g}{J_g \omega_r^2} \frac{d\omega_r}{dt} \\ a_3 &= \frac{1.5 \rho \pi R^2 v_w^2 C_p}{J_g \omega_r} \frac{dv_w}{dt} \\ a_4 &= -\frac{0.5 \rho \pi R^2 v_w^3 C_p}{J_g \omega_r^2} \frac{d\omega_r}{dt} + \frac{d^2 \omega_r}{dt^2} \\ a_5 &= \frac{0.5 \rho \pi R^2 v_w^3}{J_g \omega_r} \left( \frac{dC_p}{d\omega_r} \right) \left( \frac{d\omega_r}{dt} \right) \\ a_6 &= \frac{0.5 \rho \pi R^2 v_w^3}{J_g \omega_r} \left( \frac{dC_p}{dv_w} \right) \left( \frac{dv_w}{dt} \right) \end{aligned}$$

and  $\omega_r$  is the turbine speed. The derivatives of the  $C_p(\lambda, \beta)$  are defined in the Appendix. As can be seen in (6), the pitch angle is a nonlinear function of the wind speed, generator speed, generator power, and power conversion coefficient.

### III. EXISTING METHODS OF PITCH ANGLE CONTROL

In this section, several existing methods for pitch regulation will be described.

#### A. PI/PID Controllers

The conventional pitch control strategy uses the PI/PID controllers to regulate the rotor speed or turbine output power [14], [15], [27]. In the partial-load operation,  $\beta_{\text{ref}}$  is fixed at zero and the maximum power point tracking (MPPT) method is applied, so that the energy conversion coefficient is maximized in the partial-load region. In the full-load region, the pitch controller is activated to regulate the generator output power or speed to follow their reference values. The block diagram of the pitch angle control using the PID regulators is shown in Fig. 3, where the control variable ( $X_g$ ) is either the generator output power ( $P_g$ ) or rotational speed ( $\omega_r$ ). For the PI/PID controllers,  $K_{\text{sys}}$  is set to be 1.

To design the PI/PID controller, the nonlinear dynamics of wind turbines is linearized at a specific operating point ( $\omega_{\text{top}}$ ,  $\beta_{\text{op}}$ ,  $v_{w0}$ ), at which the turbine and generator torques are assumed to be the same. From (4) [23]

$$J_g \Delta \dot{\omega}_r = \gamma \Delta \omega_r + \alpha \Delta v_w + \delta \Delta \beta \quad (7)$$

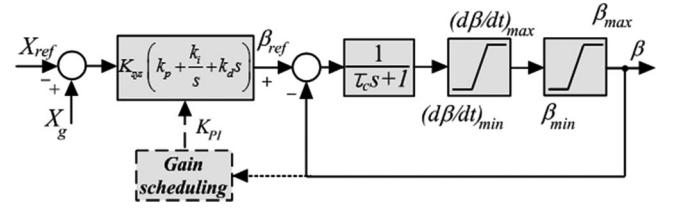


Fig. 3. Block diagram of the pitch control system using PI and PID controllers.

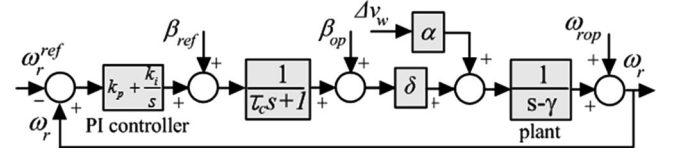


Fig. 4. Block diagram of pitch control system using PI controllers for the linearized wind turbine.

where

$$\delta = \frac{1}{2\omega_r J_g} \rho \pi R^2 v_w^3 \frac{\partial C_p(\lambda, \beta)}{\partial \beta} \quad (8)$$

$$\alpha = \frac{1}{2J_g} \rho \pi R^2 v_w \left[ 3V C_p(\lambda, \beta) + R \frac{\partial C_p(\lambda, \beta)}{\partial \lambda} \right] \quad (9)$$

$$\gamma = \frac{1}{2J_g} \rho \pi R^2 v_w^2 \left[ -\frac{1}{\omega_r^2} v_w C_p(\lambda, \beta) + \frac{R}{\omega_r} \frac{\partial C_p(\lambda, \beta)}{\partial \lambda} \right] \quad (10)$$

where  $\partial C_p(\lambda, \beta)/\partial \lambda$  and  $\partial C_p(\lambda, \beta)/\partial \beta$  are defined in the Appendix.

The block diagram of the pitch angle control system with the linearized model of the wind turbine is shown in Fig. 4, from which the variable  $\gamma$ , depicting the aerodynamic characteristics of the wind turbines, should be negative for the stability [28].

From Fig. 4, the denominator of the transfer function for  $\omega_r(s)$  can be expressed as [8], [27]

$$H(s) = \frac{s(s + (1/\tau_c))(s - \gamma) - \delta(sk_p + k_i)}{s(s + (1/\tau_c))(s - \gamma)}. \quad (11)$$

For stability, the components of the terms in the transfer function have to be positive. For instant, at the operating point, where the  $v_{w0} = 12$  (m/s),  $\omega_{\text{top}} = 16.6$  (rpm) and  $\beta_{\text{op}} = 8$  (deg), the parameters of the wind turbine are calculated from (8)–(10) as  $\alpha = 0.0207$ ,  $\delta = -0.0335$ , and  $\gamma = -0.087$ . To maintain the stability over a wide region, the proportional ( $k_p$ ) and integral ( $k_i$ ) gains need to follow as  $k_p > -1$  and  $k_i > 0$ .

As aforementioned, when the operating point is changed, the PI controller gains need to be redesigned to maintain the system dynamic response and stability.

#### B. PI Controller With Gain Scheduling

To improve the control performance of the nonlinear system, the PI controller with the gain scheduling is used. The gain scheduling for the pitch control is to compensate for the changes of the sensitivity of the aerodynamic torque to the pitch angle. The total gain of the system in the pitch control loop  $K_{\text{sys}}$ , as

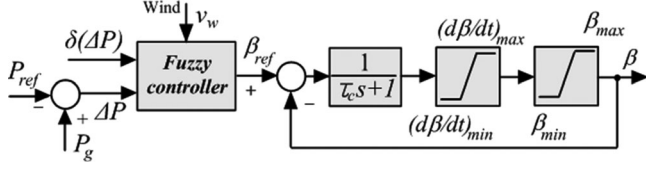


Fig. 5. Block diagram of pitch controller using fuzzy logic [23].

shown in Fig. 3, is expressed as [12]

$$K_{sys} = K_{PI} \frac{dP_{sen}}{d\beta} \quad (12)$$

where  $K_{PI}$  is the gain scheduling constant and  $dP_{sen}/d\beta$  is the aerodynamic sensitivity of the turbine, which depends on the variations of the turbine output power with the pitch angle [19], [20]. As the sensitivity of the system is higher, the controller gain is lower, and *vice versa*.

To guarantee that the pitch angle control is operated appropriately in the wide range of wind speed, the  $K_{PI}$ , which scales the proportional and integral gains is given as [12]

$$K_{PI} = \begin{cases} 1, & \text{for } (-3^\circ < \beta \leq 0^\circ) \\ \frac{\beta}{2} + 3.5, & \text{for } (0^\circ < \beta \leq 27^\circ) \\ 30, & \text{for } (\beta > 27^\circ) \end{cases} \quad (13)$$

### C. Sliding-Mode Control

The different strategies using the sliding mode control scheme have been suggested [21], [28]–[30]. This method is effective to provide the robustness to the parameter variations of the wind turbine system. However, when the control variables are changed suddenly, the stress for the system is high and the chattering phenomena are increased [31].

### D. Fuzzy Logic Controller

The FLC, in which the design of the controller is based on human experience through a set of the empirically determined design rules, has been used for controlling the pitch angle [22], [23]. The control block diagram using the fuzzy logic is shown in Fig. 5, in which the generator output power and wind speed are assigned as the control inputs of the FLC. The advantage of this method is that the parameters of the wind turbine system do not need to be known accurately. However, this method requires the wind speed information.

## IV. PROPOSED PITCH CONTROL SCHEME BASED ON FUZZY LOGIC CONTROL

The block diagram of the proposed pitch angle control based on the fuzzy logic is shown in Fig. 6. In the partial-load region, the power reference of the wind turbine  $P_{ref}$  is determined by the MPPT control strategy, which is expressed as [14], [32]

$$P_{ref} = K_{opt} \cdot \omega_r^3 \quad (14)$$

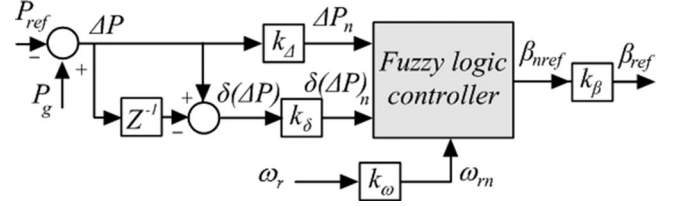


Fig. 6. Block diagram of the proposed pitch angle control with FLC.

where

$$K_{opt} = 0.5 \cdot \rho \pi C_{p \max} \frac{R^5}{\lambda_{opt}^3} \quad (15)$$

and the maximum power coefficient  $C_{p \max}$  corresponds to the optimal tip-speed ratio  $\lambda_{opt}$ , with a zero-pitch angle. In the high-wind-speed region, the  $P_{ref}$  is selected as the rated power of wind turbines. To find the pitch angle reference  $\beta_{ref}$ , the design process for a fuzzy logic controller (FLC) consists of determining the inputs, setting up the rules and converting the results of the fuzzy rules into the output signal which is known as defuzzification.

For this control scheme, the error in the generator power  $\Delta P$ , the variation of the power error  $\delta(\Delta P)$ , and the rotational speed  $\omega_r$  are considered as the controller inputs, in which the  $\Delta P$  and  $\delta(\Delta P)$  are defined as

$$\Delta P(k) = P_g(k) - P_{ref}(k) \quad (16)$$

$$\delta(\Delta P) = \Delta P(k) - \Delta P(k-1). \quad (17)$$

The pitch angle reference is considered as a controller output. The variation of the power error  $\delta(\Delta P)$ , can be calculated by (17), which is shown in Fig. 6, where the  $Z^{-1}$  represents one sampling time delay.

To design the fuzzy sets of the inputs and output, the triangular membership functions with the overlap are used, which are illustrated in Fig. 7. The linguistic variables are represented by Negative Big (NB), Negative Medium Big (NMB), Negative Medium (NM), Negative Small (NS), Zero (ZE), Positive Small (PS), Positive Medium (PM), Positive Medium Big (PMB), and Positive Big (PB).

The grade of the input membership functions is obtained from the following equation expressed as [33], [34]

$$\mu(z) = 1 - \frac{|z - m|}{0.5w} \quad (18)$$

where  $w$  is the width and  $m$  is the coordinate of the point at which the grade of the membership is 1, and  $z$  is the value of the input variable. Fig. 7 shows the values of the grade of the memberships, which are related to the values of the fuzzy control inputs.

The control rules are derived from the experience and knowledge on the control system. The fuzzy mapping of the input variables to the output is expressed by the following rules:

$R_i$ : IF  $\omega_r(k)$  is  $A_i$  and  $\Delta P(k)$  is  $B_i$  and  $\Delta P(k-1)$  is  $C_i$   
THEN  $\beta_{nref}$  is  $D_i$ .



TABLE I  
RULES OF FLC

$\omega_r$		PS					PM					PB				
$\Delta P$		NB	NS	ZE	PS	PB	NB	NS	ZE	PS	PB	NB	NS	ZE	PS	PB
$\delta\Delta P$	NB	NB	NB	NB	NB	NMB	NS	NS	NS	PM	PMB	PS	PS	PM	PMB	PB
	NS	NB	NB	NB	NMB	NMB	NS	NS	ZE	PM	PMB	PS	PS	PMB	PMB	PB
	ZE	NB	NB	NMB	NMB	NM	NS	ZE	ZE	PM	PMB	PS	PM	PMB	PB	PB
	PS	NB	NMB	NMB	NM	NM	NS	ZE	ZE	PMB	PMB	PM	PM	PB	PB	PB
	PB	NMB	NMB	NM	NM	NM	ZE	ZE	PS	PMB	PMB	PM	PM	PB	PB	PB

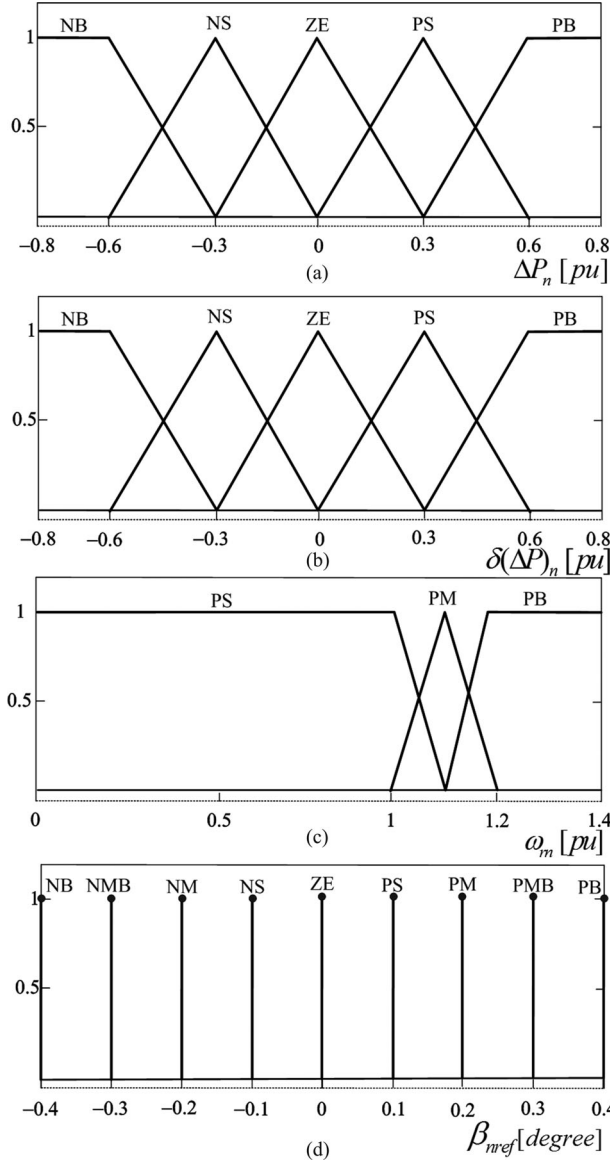


Fig. 7. Membership functions of proposed FLC for (a) error of generator output power. (b) Variation of power error. (c) Rotational speed. (d) Pitch angle reference.

where  $A_i$ ,  $B_i$ , and  $C_i$  are the fuzzy subset,  $D_i$  is a fuzzy singleton. The fuzzy rules are given in Table I.

In this paper, the fuzzy with the Sugeno type is applied for the inference mechanism [33], [34]. Each rule is weighted by the weighting factor  $W_i$  of the rule, which is obtained from the

TABLE II  
PARAMETERS OF WIND TURBINE FOR SIMULATION

Rated power	2 MW
Blade radius	38.3 m
Air density	1.225 kg/m <sup>3</sup>
Max. power conv. coefficient	0.411
Cut-in speed	3 m/s
Cut-out speed	25 m/s
Rated wind speed	12 m/s
Blade inertia	$6.3 \cdot 10^6$ kg·m <sup>2</sup>

minimum operation as

$$W_i = \min \{ \mu_{\Delta P}(\Delta P), \mu_{\delta\Delta P}(\delta(\Delta P)), \mu_{\omega}(\omega_r) \} \quad (19)$$

where  $\mu_{\Delta P}(\Delta P)$ ,  $\mu_{\delta\Delta P}(\delta(\Delta P))$ , and  $\mu_{\omega}(\omega_r)$  are the triangular membership functions of the  $\Delta P$ ,  $\delta(\Delta P)$ , and  $\omega_r$ , respectively.

The weighted average of every rule output, which expresses the variation of the pitch angle reference  $\beta_{nref}$  is calculated as [34], [35]

$$\beta_{nref} = \frac{\sum_{i=1}^N W_i D_i}{\sum_{i=1}^N W_i} \quad (20)$$

where  $N$  is the total number of the rules and  $D_i$  is the coordinate corresponding to the respective output or consequent membership function. The actual pitch angle reference is obtained from multiplying  $\beta_{nref}$  by  $k_\beta$ .

For convenience, the inputs of the FLC are normalized by the coefficients of  $k_\Delta$ ,  $k_\delta$ ,  $k_\omega$ , and  $k_\beta$ , which depend on the base value. These scaling factors can be constants or variables which play an important role in the FLC design to achieve a better response in both transient and steady states. In this work, for the simplicity of the controller design, the scaling factors ( $k_\Delta$ ,  $k_\delta$ ,  $k_\omega$ ,  $k_\beta$ ) are selected to be constant.

The stability of the proposed pitch angle control system can be guaranteed if the derivative of Lyapunov function is negative semi-definite in the active region of each fuzzy rule [36], [37]. However, the stability issue is not investigated in detail since it is beyond the scope of this research.

## V. SIMULATION RESULTS

To verify the validity of the proposed method, the simulation has been performed for 2-MW PMSG wind power system. The parameters of the wind turbine and PMSG are listed in Tables II and III, respectively. The sampling time for the FLC is 2 ms. The pitch angle rate is limited to  $\pm 10^\circ \text{ s}^{-1}$ .

Fig. 8 shows the wind speed, of which the rated value is 12 m/s. By this input wind speed, the turbine is operated in

TABLE III  
PARAMETERS OF PMSG FOR SIMULATION

Rated power	2 MW
Grid voltage	690 V
Stator voltage/frequency	690 V/16.6 Hz
Stator resistance	0.008556 $\Omega$
Stator inductance	0.00359 H
Generator inertia	48 000 kg·m <sup>2</sup>

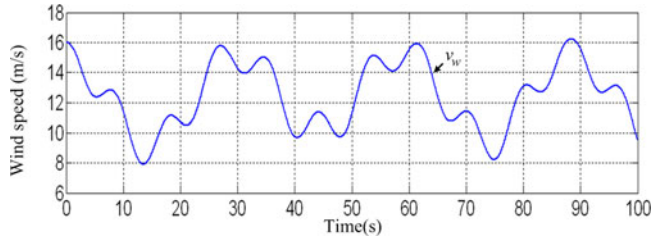


Fig. 8. Wind speed pattern.

the full-load region. The input variables for the proposed fuzzy logic control, which are the error of the generator output power, the variation of the power error, and the rotor speed, are shown in Fig. 9(a), (b), and (c), respectively. Then, the pitch angle reference is produced as shown in Fig. 9(d). With this pitch angle, the generator speed is kept at the rated value as shown in Fig. 9(c).

Fig. 10 shows the performance comparison of the three pitch angle controllers; (a) for the PI controllers with the fixed gains ( $k_p = 3$  and  $k_I = 30$ ); (b) for the PI controllers with the gain scheduling; (c) for the PID controllers with the fixed gains ( $k_p = 3$ ,  $k_I = 30$ , and  $k_d = 20$ ); (d) for the proposed control scheme with  $k_\Delta = 0.5 \times 10^{-6}$ ,  $k_\delta = 0.5 \times 10^{-2}$ , and  $k_\omega = 6 \times 10^{-2}$ ,  $k_\beta = 100$ . For the PI/PID controllers, only one variable of either the generator power or speed is used as a control input, whereas in the proposed fuzzy logic control method, both the generator power and the rotor speed are involved for the control input variables. Fig. 10(a) shows the generator power which is not well maintained at the rated value and has the high ripple components with the PI/PID controllers, whereas it is kept almost at the rated value by the proposed pitch control strategy. The average generator power for the three methods in the full-load region is evaluated, in which the proposed method gives 5.097%, 2.043%, and 3.065% higher output power than that of the PI controllers without and with the gain scheduling, and the PID controllers, respectively. Regarding the generator speed and torque, the similar performance is shown in Fig. 10(b) and (c), respectively. Fig. 10(d) shows the power conversion coefficient, which is kept at the maximum value of 0.411 for a variable speed region, however, it is decreased in the full-load region according to the increase of the pitch angle as shown in Fig. 10(e).

To investigate the performance of the PI controllers and the FLC at the different operating point, the rated wind speed which classifies the partial and full-load regions is set as 14 m/s, differently from the previous case of 12 m/s.

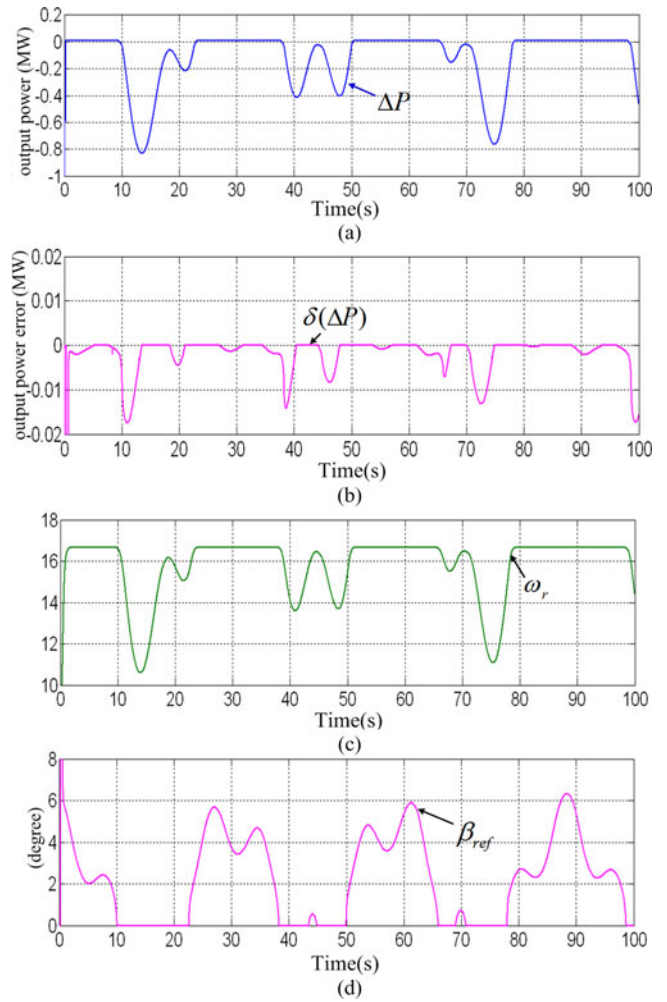


Fig. 9. Inputs and outputs of proposed FLC. (a) Error of generator output power. (b) Variation of generator output power error. (c) Rotor speed. (d) Pitch angle reference.

Fig. 11 shows the results of the pitch control for the PI controllers with the fixed gains and with the gain scheduling, the PID controllers, and the proposed fuzzy controller, at the rated wind speed of 14 m/s. The gain parameters for both the PI/PID controllers and the membership function of the fuzzy logic control are the same as those of the prior case. The wind speed pattern is the same for both cases as shown in Fig. 11(a). All of the pitch angle control methods can limit the generator power and rotor speed to their rated values. However, the pitch angle control employing the proposed fuzzy control method gives better performance than those of the PI control without and with the gain scheduling and the PID controllers. Fig. 11(b)–(d) shows the generator output power, rotor speed, and mechanical torque, respectively, where with the same controller gains, the PI controllers without and with gain scheduling, and the PID controllers at the mean wind speed of 14 m/s, cannot give as good results as that designed at the mean wind speed of 12 m/s. Meanwhile, they are kept mostly at the rated value in the high-wind-speed region with the proposed control scheme. Therefore, to guarantee that the system works well at every operating point, these gains should be redesigned. On the other hand, although

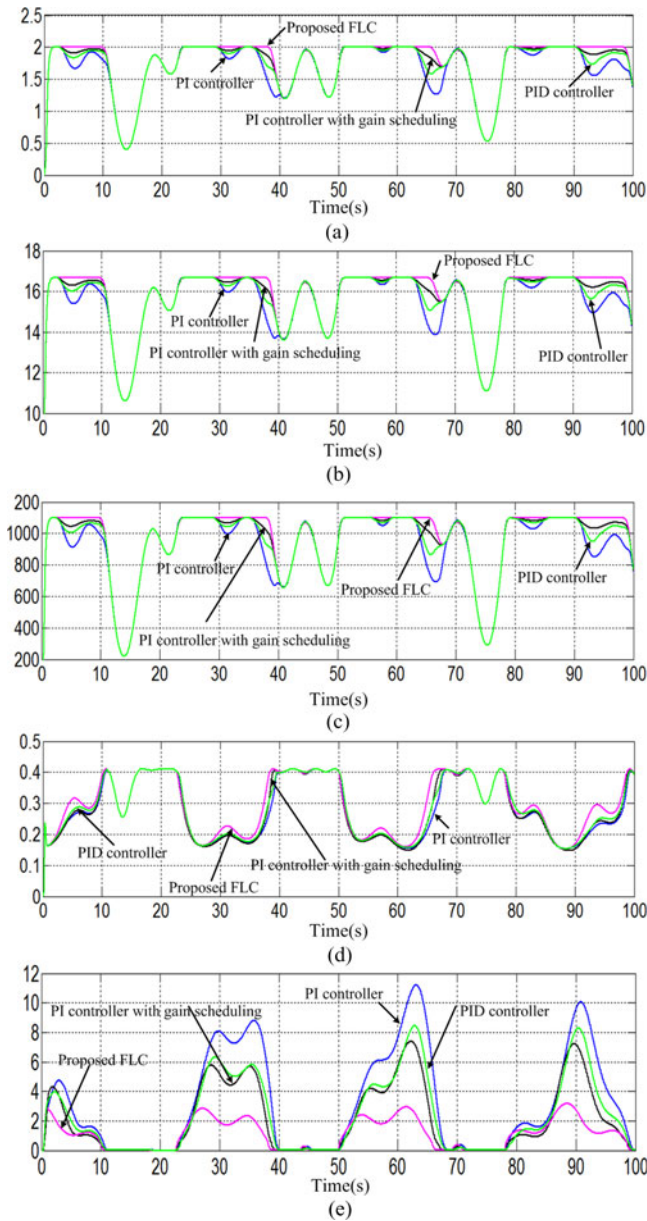


Fig. 10. Simulation results for PI controllers without and with gain scheduling, PID controllers, and proposed FLC at the mean wind speed of 12 m/s. (a) Generator powers. (b) Rotor speeds. (c) Mechanical torques. (d) Power conversion coefficients. (e) Pitch angles.

the operating point is changed, the pitch angle control using the proposed FLC method still gives good performance. It is evaluated that in the high-wind-speed region, the average generator output power with the proposed method is 2.36%, 1.07%, and 1.5% higher than that of using the PI controllers without and with the gain scheduling, and the PID controllers, respectively.

## VI. EXPERIMENTAL RESULTS

The proposed fuzzy logic scheme for pitch angle control has been also tested by experiment for a 2.68-kW PMSG wind turbine system. The layout of the experimental setup in the laboratory is shown in Fig. 12, where a squirrel-cage induction motor (SCIM) is used as a turbine simulator. The SCIM

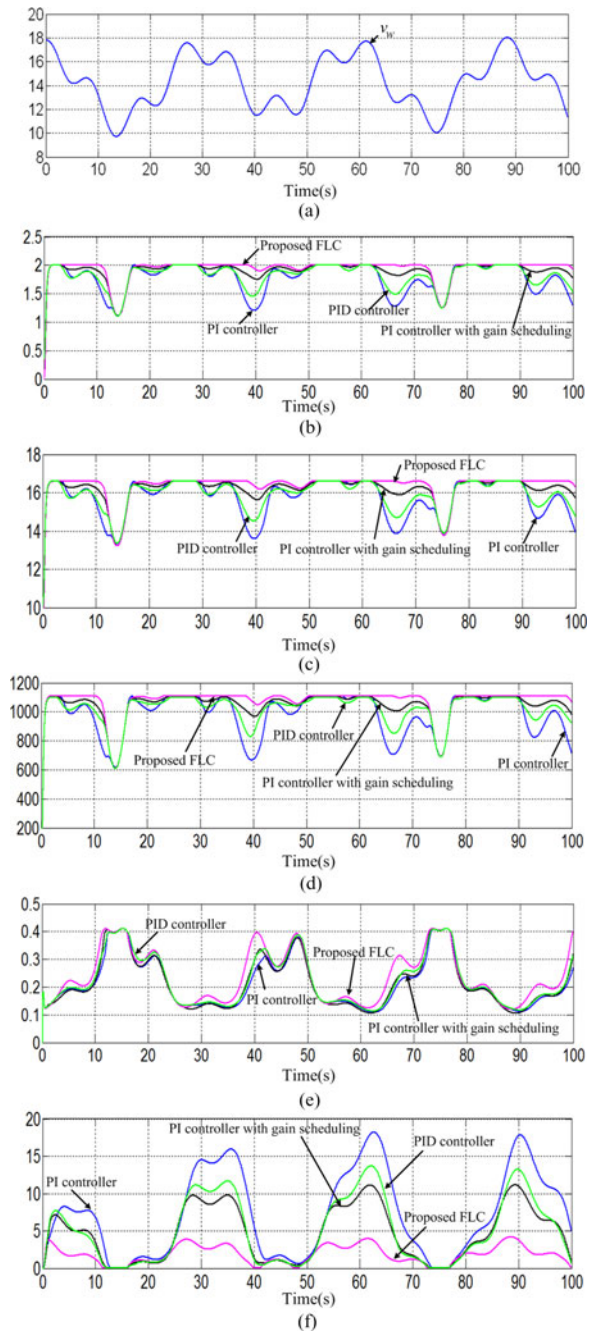


Fig. 11. Simulation results for PI controller without and with gain scheduling, PID controllers, and proposed FLC at the mean wind speed of 14 m/s. (a) Wind speeds. (b) Generator powers. (c) Rotor speeds. (d) Mechanical torques. (e) Power conversion coefficients. (f) Pitch angles.

is driven by a back-to-back converter, in which the SCIM is operated under the torque controller. The torque reference depends on the variables such as the generator speed and the wind speed, which characterizes the SCIM operation as the wind turbine. The parameters designed for the 1.8 kW wind turbine are listed in Table IV, in which the pitch angle rate is limited to  $\pm 10^\circ \text{ s}^{-1}$ . Also, the parameters of the PMSG are listed in Table V in Appendix. DSP TMS320VC33 chips with 14-bit analog-to-digital converter were used for the main board control for the PMSG and the SCIM. The grid voltage and frequency are 220



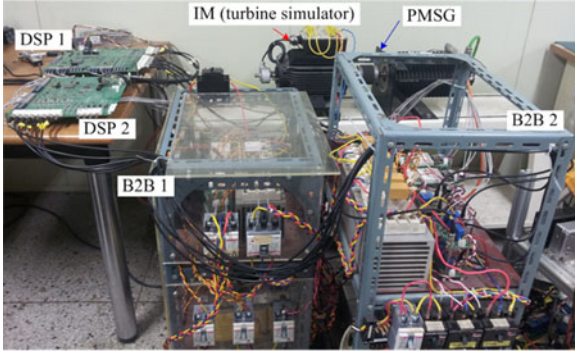


Fig. 12. Layout of experimental setup.

TABLE IV  
PARAMETERS OF DESIGNED TURBINE SIMULATOR FOR EXPERIMENT

Air density	1.225 kg/m <sup>3</sup>
Blade radius	1.16 m
Max. power conv. coefficient	0.4
Optimal tip-speed ratio	7.9
Rated wind speed	12 m/s
Blade inertia	0.00331 kg-m <sup>2</sup>

TABLE V  
PARAMETERS OF PMSG FOR EXPERIMENT

Rated power	2.68 kW
Voltage/frequency	220 V/60 Hz
Rated flux	0.468 Wb
Moment of inertia	0.00331 kg-m <sup>2</sup>
Stator resistance	0.49 $\Omega$
Stator inductance	5.35 mH
Number of poles	6

$V_{rms}$  and 60 Hz, respectively. The dc-link voltage is controlled at 340 V. The capacitance of the 1650  $\mu$ F is used for dc-link capacitor. The switching frequency is the 5 kHz. The sampling time of the current controller is 100  $\mu$ s, while the sampling time for the speed controller, torque controller, and the FLC is 1 ms.

Figs. 13 and 14 show the system performance of the pitch angle control methods, at the rated wind speed of 12 m/s, for the two controllers: (1) using the PI controller with  $k_P = 0.4$  and  $k_I = 2$ ; and (2) using the FLC with  $k_{\Delta} = 3.73 \cdot 10^{-4}$ ,  $k_{\delta} = 0.373$ ,  $k_{\omega} = 7.692 \cdot 10^{-4}$ , and  $k_{\beta} = 50$ . At the rated wind speed of 12 m/s, the rated generator speed is 1,300 rpm and the generator output power is 1.8 kW.

The wind speed patterns are the same for the two aforementioned methods as shown in Figs. 13(a) and 14(a). It is seen that both of the pitch angle control algorithms can limit the generator power and speed at the rated value during the full-load region. However, as shown in Fig. 14(b) and (c), the generator power and speed, respectively, by employing the proposed fuzzy control method, have low ripple components than those of using the PI control method as shown in Fig. 13(b) and (c), respectively, during the high-wind-speed regions. For the full-load interval of 40 s, the average generator power with the FLC is 1.38% higher than that of with the PI controller. Also, Figs. 13(d) and 14(d) show the turbine torques, in which the turbine torque using the

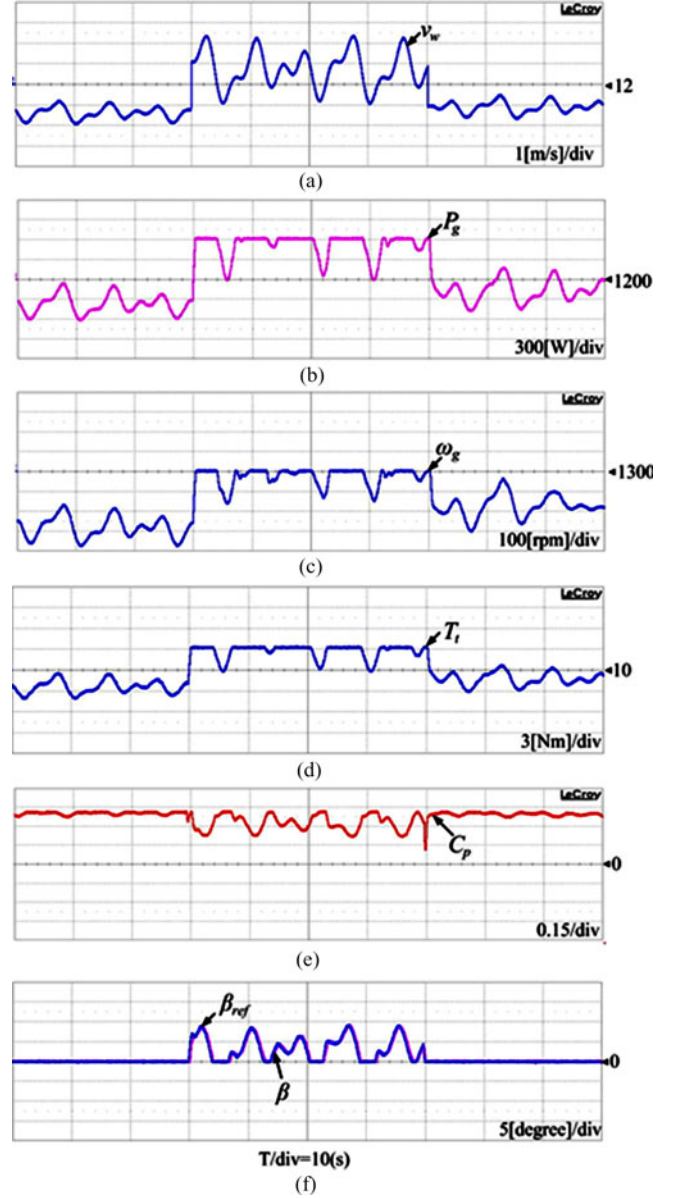


Fig. 13. Experimental results for PI controller at the rated wind speed of 12 m/s. (a) Wind speed. (b) Generator power. (c) Rotor speed. (d) Mechanical torque. (e) Power conversion coefficient. (f) Pitch angle.

proposed method reaches the rated value faster than that of using the PI control. Figs. 13(e) and 14(e) show the power conversion coefficient with the PI control and the FLC methods, in which it is kept at the maximum value at about 0.41 in the partial-load region. Also, regarding the pitch angle as shown in Figs. 13(f) and 14(f), both cases are varied to maintain the generator power and speed at their rated values.

## VII. CONCLUSION

In this research, a novel pitch control scheme employing the fuzzy logic control for the PMSG wind turbine system has been proposed to limit the turbine output power and the turbine speed at their ratings. To develop the control scheme, the nonlinear characteristics of pitch system have been derived, which is based



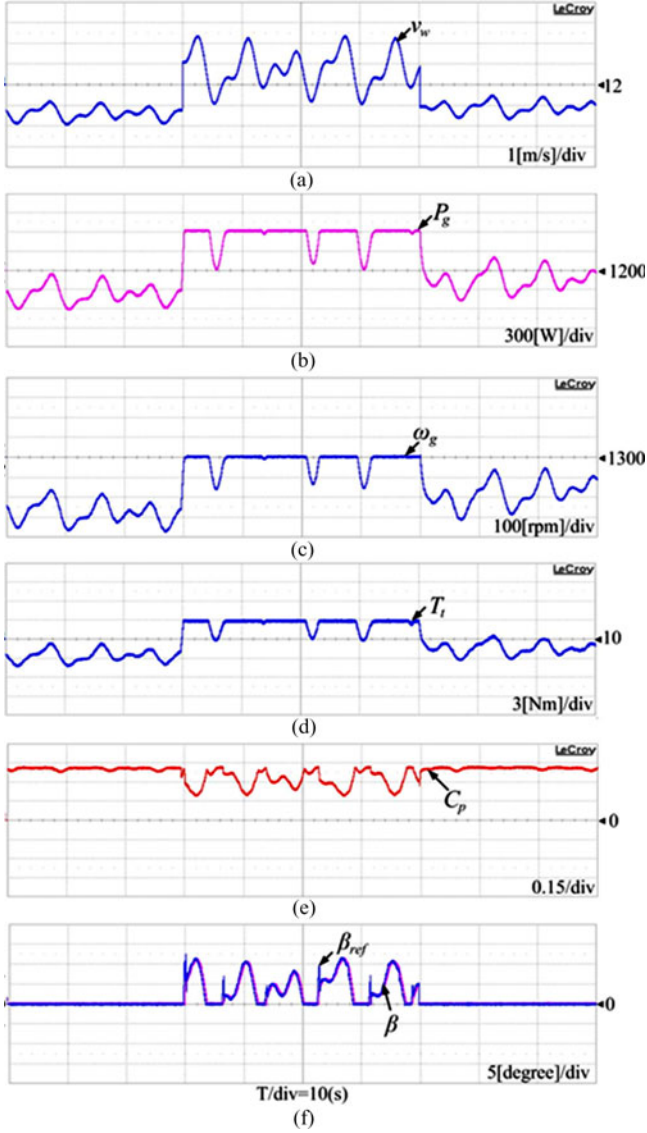


Fig. 14. Experimental results for proposed FLC at the rated wind speed of 12 m/s. (a) Wind speed. (b) Generator power. (c) Rotor speed. (d) Mechanical torque. (e) Power conversion coefficient. (f) Pitch angle.

on small signal analysis. Then, the rotational speed and generator output power are selected as the control input variables of the FLC, in which any information of the wind turbine dynamics and the wind speed is not necessary. The simulation and experimental results have illustrated that the proposed pitch angle controller can regulate the turbine output power and speed at the rated values satisfactorily at high-wind-speed regions.

#### APPENDIX

The derivatives of the  $C_p(\lambda, \beta)$  are expressed as

$$\frac{dC_p(\lambda, \beta)}{d\lambda} = \frac{c_1}{(\lambda + 0.08\beta)^2} e^{-\frac{c_6}{\lambda}} \left\{ -c_2 + \frac{c_2 c_6}{\lambda} - c_3 c_6 \beta - c_5 c_6 \right\}$$

$$\frac{dC_p(\lambda, \beta)}{d\beta} = c_1 e^{-\frac{c_6}{\lambda}} \left\{ \frac{d}{d\beta} \left( \frac{1}{\lambda} \left( c_2 + c_5 c_6 - \frac{c_2 c_6}{\lambda} + c_3 c_6 \beta \right) - c_3 \right) \right\}$$

where

$$\frac{d}{d\beta} \frac{1}{\lambda} = -\frac{0.08}{(\lambda + 0.08\beta)^2} + \frac{0.035 \cdot 3\beta^2}{(\beta^3 + 1)^2}$$

$$\begin{aligned} \frac{dC_p(\lambda, \beta)}{d\omega_g} &= -\frac{c_1 \frac{R}{v_w}}{\left( \frac{\omega_g R}{v_w} + 0.08\beta \right)^2} e^{-\frac{c_6}{\lambda}} \\ &\times \left\{ c_2 - \frac{c_2 c_6}{\lambda} + c_3 c_6 \beta + c_5 c_6 \right\} \\ \frac{dC_p(\lambda, \beta)}{dv_w} &= c_1 \left\{ \frac{R\omega_g}{v_w^2 (\lambda + 0.08\beta)^2} \right\} e^{-\frac{c_6}{\lambda}} \\ &\times \left\{ c_2 - \frac{c_2 c_6}{\lambda} + c_3 c_6 \beta + c_5 c_6 \right\}. \end{aligned}$$

The parameters of wind turbine and generators using for simulation and experiment are shown in Tables II–V, respectively.

#### REFERENCES

- [1] V. Akhmatov, "Analysis of dynamic behavior of electric power systems with large amount of wind power," Ph.D. dissertation, Dept. Elect. Eng., Tech. Univ. Denmark, Kgs. Lyngby, Denmark, Apr. 2003.
- [2] T. H. Nguyen, D.-C. Lee, T. L. Van, and J.-H. Kang, "Coordinated control of reactive power between STATCOMs and wind farms for PCC voltage regulation," *J. Power Electron.*, vol. 13, no. 5, pp. 909–918, Sep. 2013.
- [3] A. Bechouche, D. O. Abdeslam, T. O. Cherif, and H. Seddiki, "Adaptive neural PLL for grid-connected DFIG synchronization," *J. Power Electron.*, vol. 14, no. 3, pp. 608–620, May 2014.
- [4] Y. Zhang, Z. Chen, W. Hu, and M. Cheng, "Flicker mitigation by individual pitch control of variable speed wind turbines with DFIG," *IEEE Trans. Energy Convers.*, vol. 29, no. 1, pp. 20–28, Mar. 2014.
- [5] N. P. W. Strachan and D. Jovicic, "Improving wind power quality using an integrated wind energy conversion and storage system (WECSS)," in *Proc. IEEE Power Energy Soc. Gen. Meeting*, Jul. 2008, pp. 1–6.
- [6] Y. Nam, P. T. Kien, and Y.-H. La, "Alleviating the tower mechanical load of multi-MW wind turbines with LQR control," *J. Power Electron.*, vol. 13, no. 6, pp. 1024–1031, Nov. 2013.
- [7] N. Horiuchi and T. Kawahito, "Torque and power limitations of variable speed wind turbines using pitch control and generator power control," in *Proc. IEEE Power Eng. Soc. Summer Meeting*, vol. 1, 2001, pp. 638–643.
- [8] S. Roy, "Power output by active pitch-regulated wind turbine in presence of short duration wind variations," *IEEE Trans. Energy Convers.*, vol. 28, no. 4, pp. 1018–1025, Dec. 2013.
- [9] D. J. Leith and W. E. Leighead, "Implementation of wind turbine controllers," *Int. J. Control*, vol. 1, pp. 349–380, 1997.
- [10] T. Senjyu, R. Sakamoto, N. Urasaki, T. Funabashi, H. Fujita, and H. Sekine, "Output power leveling of wind turbine generator for all operating regions by pitch angle control," *IEEE Trans. Energy Convers.*, vol. 21, no. 2, pp. 467–475, Jun. 2006.
- [11] R. M. Kamel, A. Chaouachi, and K. Nagasaka, "Wind power smoothening using fuzzy logic pitch controller and energy capacitor system for improvement micro-grid performance in islanding mode," *Energy*, vol. 35, no. 5, pp. 2119–2129, Mar. 2010.
- [12] M. M. Hand, "Variable-speed wind turbine controller systematic design methodology: A comparison of nonlinear and linear model-based designs," National Renewable Energy Laboratory, Golden, CO, USA, NREL Rep. TP-500-25540, Jul. 1999.
- [13] L. Qu and W. Qiao, "Constant power control of DFIG wind turbines with supercapacitor energy storage," *IEEE Trans. Ind. Appl.*, vol. 47, no. 1, pp. 359–367, Jan./Feb. 2009.

- [14] A. O. Ibrahim, T. H. Nguyen, D.-C. Lee, and S.-C. Kim, "A fault ride-through technique of DFIG wind turbine systems using dynamic voltage restorers," *IEEE Trans. Energy Convers.*, vol. 26, no. 3, pp. 871–882, Sep. 2011.
- [15] A. Uehara, A. Pratap, T. Goya, T. Senjyu, A. Yona, N. Urasaki, and T. Funabashi, "A coordinated control method to smooth wind power fluctuations of a PMSG-based WECS," *IEEE Trans. Energy Convers.*, vol. 26, no. 2, pp. 550–558, Jun. 2011.
- [16] R. Sakamoto, T. Senjyu, T. Kaneko, N. Urasaki, T. Takagi, S. Sugimoto, and H. Sekine, "Output power leveling of wind turbine generator by pitch angle control using  $H_\infty$  control," in *Proc. IEEE PES Power Syst. Conf. Expo.*, Oct. 2006, pp. 2044–2049.
- [17] T. Ekelund, "Speed control of wind turbines in the stall region," *Proc. 3rd IEEE Conf. Control Appl.* 1994, pp. 227–232.
- [18] U. Shaked and E. Soroka, "On the stability robustness of the continuous time LQG optimal control," *IEEE Trans. Autom. Control*, vol. AC-30, no. 9, pp. 1039–1043, Oct. 1985.
- [19] E. B. Muhando, T. Senjyu, A. Uehara, and T. Funabashi, "Gain-scheduled  $H_\infty$  control for WECS via LMI techniques and parametrically dependent feedback Part II: Controller design and implementation," *IEEE Trans. Ind. Electron.*, vol. 58, no. 1, pp. 57–65, Jan. 2011.
- [20] E. B. Muhando, T. Senjyu, A. Uehara, T. Funabashi, and C.-H. Kim, "LQG design for megawatt-class WECS with DFIG based on functional model's fidelity prerequisites," *IEEE Trans. Energy Convers.*, vol. 24, no. 4, pp. 893–904, Dec. 2009.
- [21] S.-H. Lee, Y. Joo, J. Back, J.-H. Seo, and I. Choy, "Sliding mode controller for torque and pitch control of PMSG wind power systems," *J. Power Electron.*, vol. 11, no. 3, pp. 342–349, May 2011.
- [22] J. Zhang, M. Cheng, Z. Chen, and X. Fu, "Pitch angle control for variable speed wind turbines," in *Proc. 3rd Int. Conf. DRPT*, 2008, pp. 2691–2696.
- [23] S. M. Mueen, J. Tamura, and T. Murata, *Stability Augmentation of a Grid-Connected Wind Farm*. Berlin, Germany: Springer-Verlag, Oct. 2008.
- [24] H. Li, K. L. Shi, and P. G. McLaren, "Neural-network-based sensorless maximum wind energy capture with compensated power coefficient," *IEEE Trans. Ind. Appl.*, vol. 41, no. 6, pp. 1548–1556, Nov./Dec. 2005.
- [25] Z. Lubosny, *Wind Turbine Operation in Electric Power System*. Berlin, Germany: Springer-Verlag, 2003.
- [26] B. Boukhezzer, L. Lupu, H. Siguerdidjane, and M. Hand, "Multivariable control strategy for variable speed variable pitch wind turbines," *Renewable Energy*, vol. 32, no. 8, pp. 1273–1287, 2007.
- [27] E. A. Bossanyi, "The design of closed loop controllers for wind turbines," *Wind Energy*, vol. 3, pp. 149–163, 2000.
- [28] B. Beltran, T. Ahmed-Ali, and M. E. H. Benbouzid, "Sliding mode power control of variable speed wind energy conversion systems," *IEEE Trans. Energy Convers.*, vol. 23, no. 2, pp. 551–558, Jun. 2008.
- [29] B. Beltran, T. Ahmed-Ali, and M. E. H. Benbouzid, "High order sliding mode control of variable speed wind turbines," *IEEE Trans. Ind. Electron.*, vol. 56, no. 9, pp. 3314–3321, Sep. 2009.
- [30] L. Y. Yang, J. H. Liu, C. L. Wang, and G. F. Du, "Sliding mode control of three-phase four-leg inverters via state feedback," *J. Power Electron.*, vol. 14, no. 5, pp. 1028–1037, Sep. 2014.
- [31] P. Parida, "A sliding mode controller for induction motor," Master dissertation, National Inst. Technology, Rourkela, India, May 2009.
- [32] S. M. Barakati, M. Kazerani, and D. Aplevich, "Maximum power tracking control for a wind turbine system including a matrix converter," *IEEE Trans. Energy Convers.*, vol. 24, no. 3, pp. 705–713, Sep. 2009.
- [33] M. E. El-Hawary, *Electric Power Applications of Fuzzy Systems*. Piscataway, NJ, USA: IEEE Press, 1998.
- [34] B. K. Bose, *Modern Power Electronics and AC Drives*. Knoxville, TN, USA: Tennessee Univ./Prentice-Hall, 2002, ch. 11.
- [35] S. M. Mueen, R. Takahashi, T. Murata, and J. Tamura, "Integration of an energy capacitor system with a variable-speed wind generator," *IEEE Trans. Energy Convers.*, vol. 24, no. 3, pp. 740–749, Sep. 2009.

- [36] M.-L. Tomescu, "Stability analysis method for fuzzy control systems dedicated controlling nonlinear processes," *Acta Polytech. Hungarica*, vol. 4, no. 3, pp. 127–141, 2007.
- [37] J.-C. Lo and Y.-M. Chen, "Stability issues on Takagi-Sugeno fuzzy model-parametric approach," *IEEE Trans. Fuzzy Syst.*, vol. 7, no. 5, pp. 597–607, Oct. 1999.



**Tan Luong Van** (S'11–M'14) was born in Vietnam. He received the B.S. and M.S. degrees in electrical engineering from Ho Chi Minh City University of Technology, Ho Chi Minh City, Vietnam, in 2003 and 2005, respectively, and the Ph.D. degree in electrical engineering from Yeungnam University, Gyeongsan, Korea, in 2013.

He is currently a Lecturer in the Department of Electrical and Electronic Engineering, Sai Gon University, Ho Chi Minh City. His current research interests include power converters, machine drives, wind

power generation, power quality, and power system.



**Thanh Hai Nguyen** (S'09–M'14) was born in Dong Thap, Vietnam. He received the B.S. degree in electrical engineering from the Ho Chi Minh City University of Technology, Ho Chi Minh City, Vietnam, in 2003, and the M.S. and Ph.D. degrees in electrical engineering from Yeungnam University, Gyeongbuk, Korea, in 2010 and 2013, respectively.

He is currently a Research Professor at Yeungnam University. He was an Assistant Lecturer in the College of Technology, Can Tho University, Can Tho, Vietnam, from May 2003 to February 2008. His current

research interests include power converters, machine drives, high voltage dc transmission systems, and wind power generation.



**Dong-Choon Lee** (S'90–M'94–SM'13) received the B.S., M.S., and Ph.D. degrees in electrical engineering from Seoul National University, Seoul, Korea, in 1985, 1987, and 1993, respectively.

He was a Research Engineer with Daewoo Heavy Industry, Korea, from 1987 to 1988. Since 1994, he has been a Faculty Member in the Department of Electrical Engineering, Yeungnam University, Gyeongbuk, Korea. As a Visiting Scholar, he joined the Power Quality Laboratory, Texas A&M University, College Station, TX, USA, in 1998; the

Electrical Drive Center, University of Nottingham, Nottingham, U.K., in 2001; the Wisconsin Electric Machines and Power Electronic Consortium, University of Wisconsin–Madison, WI, USA, in 2004; and the FREEDM Systems Center, North Carolina State University, Raleigh, North Carolina, USA, from September 2011 to August 2012. His current research interests include ac machine drives, the control of power converters, wind power generation, and power quality.

Dr. Lee is currently the Editor-in-Chief for the *Journal of Power Electronics* of the Korean Institute of Power Electronics.